THE USE OF THERMAL MISMATCH STRESSES TO DETECT DISBOND INITIATION AND PROPAGATION IN METAL/COMPOSITE BONDED JOINTS USING A CFBG FIBRE OPTICAL SENSOR

Tobias F Capell[1], Stephen L Ogin[1], Andrew D Crocombe[1], Graham T Reed[2], Anthony M Thorne[1], Jayanthi Palaniappan[1], Swee Chuan Tjin[3] and Lipi Mohanty[3]
[1]School of Engineering, University of Surrey, GU2 7XH, UK
[2]School of Electronics and Physical Sciences, University of Surrey, GU2 7XH, UK
[3]School of Electrical and Electronic Engineering, Photonics Research Centre, Nanyang Technological University, Singapore

Email: S.Ogin@surrey.ac.uk

Keywords: *Adhesively bonded joints, disbond, chirped fibre Bragg grating*

Abstract

Chirped fibre Bragg grating (CFBG) sensors have been used to monitor the initiation and propagation of disbonds in composite/metal bonded joints. The CFBGs were embedded in the glass fibre reinforced plastic (GFRP) adherend of GFRP/aluminium single lap joints (SLJs), which were bonded at elevated temperature. Cooling a SLJ to room temperature resulted in a residual elastic strain due to the different coefficients of thermal expansion of the adherends. SLJs were fatigue loaded, with the CFBG sensor being interrogated at intervals using a broadband light source and a spectrum analyser when the SLJ was in an unloaded state. It was found that the relaxation of the elastic strain due to disbonding caused perturbations in the reflected spectrum from the CFBG sensors which enabled the position of the disbond front to be determined. The experimental results have been modelled using a combination of finite-element analysis and commercial software for predicting FBG spectra.

1 Introduction

Adhesively bonded joints offer many advantages over mechanical fasteners and are becoming more widely used. They provide a larger areas over which the two adherends are joined and do not require holes or other stress concentrating features. One deficiency with bonded joints in structures is the difficulty associated with confirming a joint has been properly bonded and inspecting the joint for damage in service, namely joint disbonding (also called delamination).

Several techniques are available to examine joints in situ. Ultrasonic C-scan is an established method of non-destructive testing (NDT), using the liquid coupled technique and, more recently, air transmission. For larger embedded structures (for example bridges), air transmission is the only practical way of conducting the C-scan, but because of the acoustic impedance ratio between air and composites, the amount of energy transferred to the structure is low [1], requiring powerful transducers. The technique is usually applied as a transmission through the material, which also necessitates access to both sides of the surface being examined. The technique has high sensitivity to damage of many types: disbonds, delaminations and even deformation of honeycomb structures, indeed any deformation that attenuates the transmission in relation to the surrounding undamaged structure.

Pulse thermography has been shown to be effective in detecting defects in bonded joints [2] and plastic welded joints [3]. The technique can be used on both metal and composite structures, normally requiring no surface pre-treatments and single-sided access. Thermography is a quick technique, with pulse duration varying from fractions of a second to seconds, depending on the nature of the material being examined. Disbonds can be readily detected where there is a separation

between the two adherends. Kissing bonds, where the adherends have not been bonded or have disbonded but are in very close contact, cannot usually be detected by thermography. Recent work on passive thermography to detect fretting damage in riveted joints [4] has potential for use in bonded joints to detect kissing bonds, but requires the joint to be fatigue loaded to cause the thermal emission, which itself can cause detection problems due to the thermo elastic effect.

Acoustic emission has also been applied successfully to the detection of damage in structures. An example of this is the VIGILANT system developed, in part, by Airbus. The system can detect cracks within structures in service and the monitoring of bonded joints has been investigated [5].

Optical sensors based on the fibre Bragg grating (FBG) have been shown to be able to detect many forms of damage in composites. The optical fibres are low weight and immune from electro-magnetic interference. Measurement frequencies of 100Hz are possible and multiple sensors can be written in a single fibre. The fibres are normally embedded within the composite laminate, but can be adhered to the surface [6]. The sensors are very sensitive to strain changes which affect the wavelength of the radiation reflected from the grating. The magnitude of the local strain can either be found from the change in the reflected wavelength, or the shape of the reflected spectrum can be used to detect damage. The FBG has a linear strain response, with a sensitivity which depends on the grating period and the length of the grating. Embedded fibres have been used, for example, to monitor disbonds in marine T-joints, where a bulkhead is bonded to the hull [7].

Another type of FBG, the chirped fibre Bragg grating (CFBG) has also been used to detect damage. This sensor reflects a wide band of wavelengths due to a linear increase of the grating period over the length of the sensor, allowing the position of any strain anomaly to be established by its position within the spectrum [8]. Yashiro *et al* [9] have recently used an embedded CFBG to identify different types of damage within composite structures, using the shape of the reflected spectrum to establish whether the damage had the form of a delamination or a split. In bonded structures, CFBGs have been used to monitor the initiation and growth of disbonds in single lap joints (SLJs) where both adherends are composites laminates [10]. The CFBG was embedded in one of the glass fibre reinforced plastic (GFRP) adherends and disbonds that grew under fatigue loading were monitored. The joints were statically loaded to create a strain difference between the bonded section of the joint and the section that had disbonded.

In metal/composites joints, the two adherends have different coefficients of thermal expansion. If the bond is made at elevated temperature, when the joint cools, there will be strains locked into the material that can be used instead of static loading to detect damage in the joint [11]. This paper presents results on disbond detection in metal/composite SLJs that use the locked in strains to monitor the progress of disbond growth in unloaded bonded joints, together with predictions of the results.

2 Materials and experimental methods

The metal/composite joints used in the study were made from GFRP laminates and aluminium. The GFRP was manufactured using a liquid impregnation technique on a dry frame wound pre-form; the composite adherends had a $(0_2/90/0_6)_s$ lay-up. The pre-form used 600Tex E-glass as the reinforcement fibres and the optical fibre incorporating the CFBG sensor was positioned in the pre-form during the winding process. This was accomplished by bolting two thin plastic strips to the frame prior to the final zero degree reinforcement being wound. The optical fibre was bonded between these strips using silicone rubber with the fibre running parallel to the zero degree reinforcement. The thin plastic strips remain in the composite panel after manufacture, but lie outside the grips and do not affect the tests. The liquid matrix used was an epoxy with a composition by weight of 100 parts of Bisplenol A Epicholorohydrin resin 300; 60 parts of MNA hardener and 4 parts of Ancamine K61B catalyser. The ply thickness was 0.25 mm and the optical fibre was placed adjacent to the first 0/90 interface, at approximately 0.5 mm from the surface.

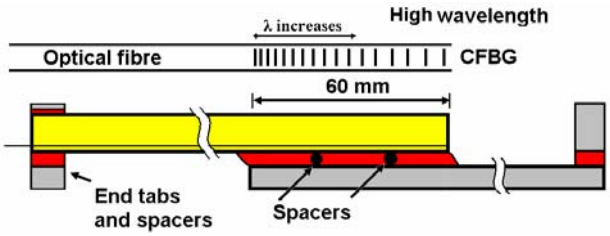

Fig. 1 A schematic of the bonded joint

Coupons were cut from the composite panel having dimensions of 145 mm x 20 mm x 4.5 mm. Each coupon had a 60 mm CFBG embedded approximately centrally within the width of the coupon with the high wavelength end of the CFBG located at the cut end. Aluminium coupons having a thickness of 1.94 mm were cut to the same length and width from sheet of 1000 series plate (UTS 131 MPa); these were degreased and etched in a chromic bath for 30 minutes. The aluminium was bonded to the GFRP using a single-part heat curing epoxy adhesive (AV119). Two 0.4 mm wires were included in the central part of the 60 mm overlap length to maintain an even bond thickness and the joint was cured at 120°C for one hour. End tabs and spacers were bonded to the ends of the SLJ to relieve bending stresses while loading. Figure 1 shows a schematic of the joint.

The CFBG sensors were 60 mm in length with a full width reflected spectra at half the maximum of 20 nm. The low wavelength end of the CFBG coincided with the termination of the aluminium adherend and the high wavelength end was adjacent to the cut end of the GFRP adherend (see figure 1). The coating of the optical fibre sensors was removed during the manufacture of the grating and was not replaced, enabling direct contact between the cladding of the optical fibre and the epoxy matrix of the composite. The optical interrogation system is shown in figure 2 and further details can be found in [10].

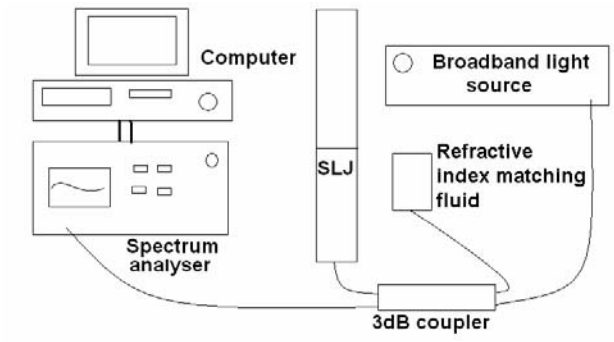

Fig. 2 The optical system

The bonded joints were fatigue loaded using an Instron servo-hydraulic testing machine under computer control. The loading was applied using a sinusoidal waveform with a peak load of 5.5 kN (42.7 MPa in the joint) and an R value ($\sigma_{max}/\sigma_{min}$) of 0.1 for 3000 cycles (this was reduced to 1000 cycles if the disbond grew quickly). After fatigue cycling, a photograph was taken of the unloaded joint to determine the disbond position and to record the CFBG spectrum.

Photographs were taken by lighting the SLJ from the front through the GFRP adherend and using a polarising filter to reduce the glare. Digital images were transferred to the computer where the contrast and brightness could be adjusted to enable the extent of the disbonding to be seen clearly through the transparent GFRP.

3 Results and discussion

3.1 Strains caused by bonding

The adhesive bonding of the joint took place at elevated temperature, 120°C, and on cooling, thermal strains develop in the adherends. The reflected spectrum from the CFBG was recorded both before bonding and after the SLJ cooled to room temperature (20°C). Figure 3 shows that the entire CFBG spectrum shifts to lower wavelengths after cooling the bonded joint to room temperature and the shift to lower wavelengths signifies a compressive strain within the GFRP adherend. This is caused by elastic stress resulting from the different coefficients of thermal expansion of the two adherends. The aluminium has a higher coefficient of thermal expansion than the GFRP laminate and imposes a compressive strain on the GFRP adherend and the embedded sensor.

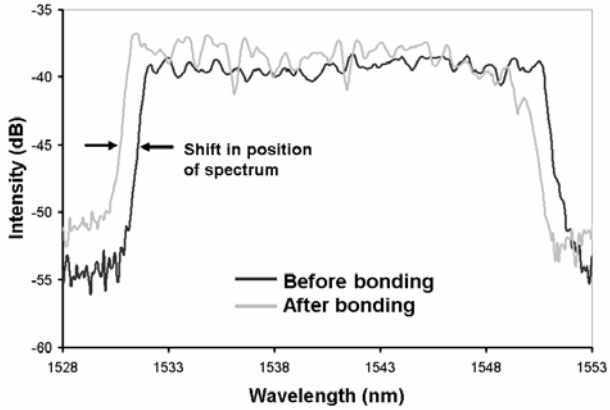

Fig. 3 The shift in the spectrum after bonding

The magnitude of the compressive strain locked into the joint can be measured from the shift in the spectrum. In the above figure, the wavelength shift is approximately 0.81 nm. The sensitivity of the 60 mm CFBGs used in this study is approximately 1 x 10^{-3} nm/με [12] and so the experimentally measured strain in the joint parallel

to the lengthwise direction of the adherends, is a compressive strain of about 810 με.

A simple one dimensional model was used to confirm the magnitude of this shift, based on the calculation of the coefficient of thermal expansion of a bi-material strip. The strain in a bi-material strip is given in Eq. 1,

$$\varepsilon = \frac{\delta l'}{l} = \Delta T\left(\frac{bE_1\alpha_1 + dE_2\alpha_2}{E_1 b + E_2 d}\right) \qquad (1)$$

where E_1, E_2, α_1,α_2, b and d are Young's moduli, coefficients of thermal expansion and thicknesses of adherend 1 and 2 respectively, and ΔT is the change in temperature.

The 0^o and 90^o plies of the GFRP laminate have coefficients of thermal expansion (CTEs) of 6.7 x 10^{-6} and 29.3 x 10^{-5} K^{-1}, respectively. The CTE of the laminate is found to be 7.54 x 10^{-6} K^{-1} which is then used to calculate the CTE of the assembled joint, 1.44 x 10^{-5} K^{-1}, using a CTE for aluminium of 2.35 x 10^{-5} K^{-1}. Using the CTE of the SLJ and a temperature change of -90 K, the total strain locked into the joint is calculated to be -1293 με. The CFBG measures the elastic strain in the GFRP adherend, where the elastic strain is the total strain minus the thermal strain. The thermal strain in the GFRP can be calculated from its CTE multiplied by the temperature change (-679 με) giving an elastic strain experienced by the sensor of -614 με. This corresponds to a predicted wavelength shift of 0.61 nm, compared to the measured value (figure 3) of 0.81 nm. The difference between the measured and predicted values is due to the simplicity of the model and also the assumption in the model that the strain is uniform along the whole joint, which is not the case in the real joint. The finite element model described later (section 3.3) predicts a shift which is in much better agreement with the experimental result.

3.2 Disbond initiation and propagation

The photographs in figure 4 show the progress of a disbond growing between the GFRP and the adhesive layer as a function of the number of fatigue cycles The optically transparent GFRP enables the progress of the disbond to be directly measured from these images and compared to the progress of the disbond as measured by the embedded optical sensor.

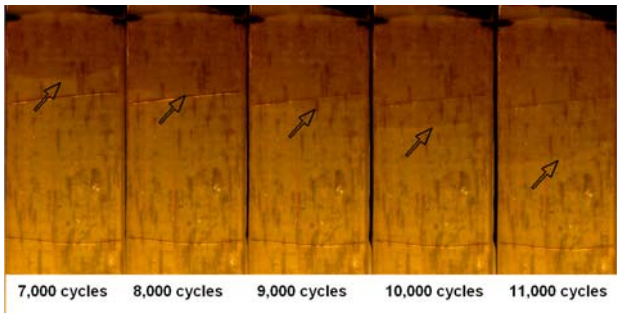

Fig. 4 Disbond progression with increasing cycles

When a disbond initiates at the low wavelength end of the CFBG sensor, the reflected spectrum from the unloaded SLJ shows a shift at the low wavelength end of the spectrum, figure 5. The mechanism behind this shift is an elongation of the grating spacings at the low wavelength end of the CFBG, caused by the GFRP being relieved of the compressive strain locked in during bonding.

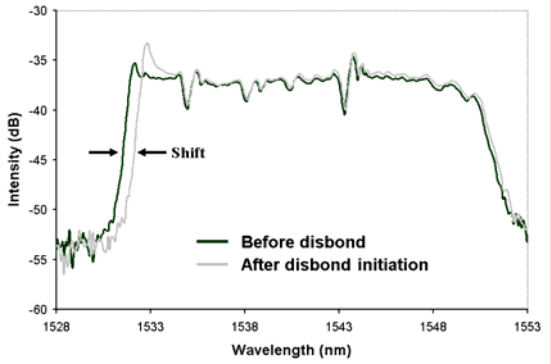

Fig. 5 Shift in spectrum indicating initiation of a disbond

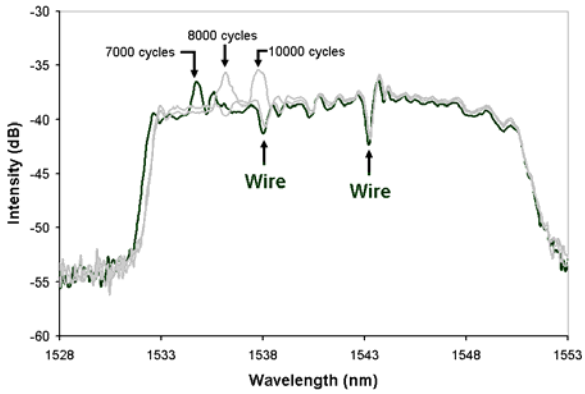

Fig. 6 Progression of the disbond in reflected spectra when growing from the low wavelength end

As the disbond grows, the position of the disbond front can be tracked by a peak in the spectrum, as shown in figure 6 which shows three spectra for an increasing length of disbond. The

peak is an increase in the intensity of reflected light of particular wavelengths. The gratings in the locality of the disbond front are relaxed and reflect a longer wavelength, the same as that reflected by gratings still within the compressed GFRP just ahead of the disbond front. This increase in the density of gratings with the same period causes the increase in reflected intensity.

When a disbond grows from the high wavelength end of the spectrum, the progress of the disbond can be traced by the position of a dip in the spectra. Figure 7 shows the progress of such a disbond with increasing numbers of cycles.

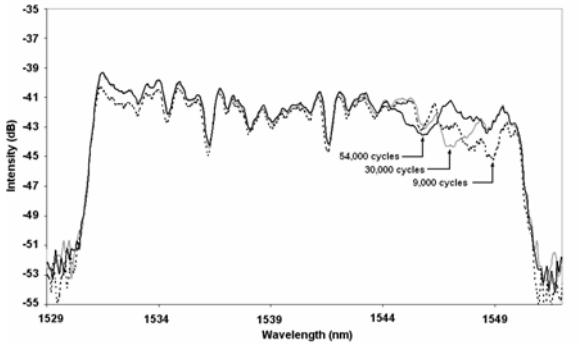

Fig. 7 Progression of disbond in reflected spectra when growing from the high wavelength end

The dip is caused by a reduction in the density of gratings of a particular period that reflect that wavelength of light. At the high wavelength end, this is caused by gratings in the disbonded region having increased periods and hence reducing the local grating density and reflected intensity.

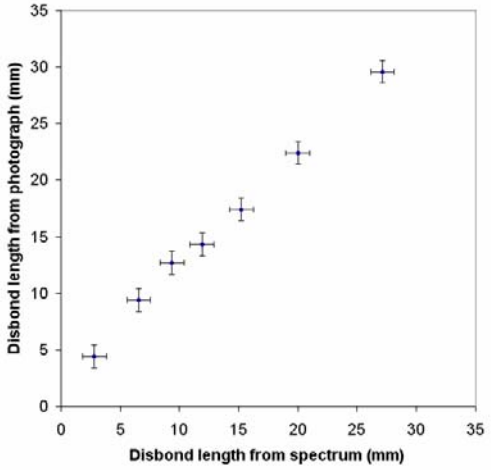

Fig. 8 Length of disbond as measured from photograph compared to length measured by CFBG at the low wavelength end

Figures 8 and 9 show comparisons between the disbond length, measured using the photographs and those measured using CFBG sensors for disbonds starting from the low and high wavelength ends, respectively. The results from the CFBG sensors have been interpreted using information from the numerical model in relation to the perturbations in the spectra (see section 3.3) in order to define the position of the disbond front. The figures show that the CFBG can be used to measure the position of the disbond front with an accuracy of about 2 mm.

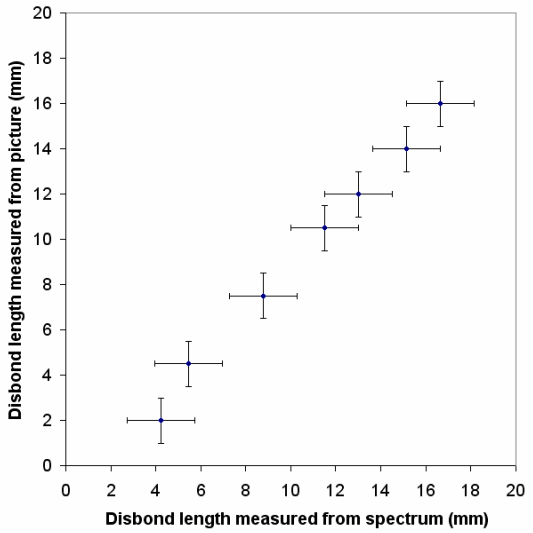

Fig. 9 Length of disbond as measured from photograph compared to length measured by CFBG at the high wavelength end

3.3 Numerical model and predicted spectra

The SLJ has been modelled using ABAQUS (version 6.6-1). The model is a two dimensional representation of the joint, analysed using generalised plane strain conditions. The joint is modelled as a multi layer composite bonded to the aluminium. The spacing wires are omitted, as are the end tabs and spacers. The adhesive is cut square with the end of the adherend (i.e. there is no adhesive fillet) and the optical fibre is not modelled explicitly. The SLJ is pinned at the end of the GFRP adherend to prevent movement within the analysis environment. Joints are analysed thermally by imposing a uniform temperature drop.

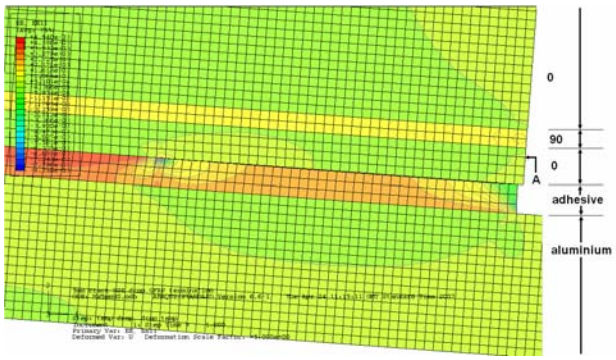

Fig. 10 Magnified image of the deformed SLJ with a 5 mm disbond starting at the termination of the GFRP adherend

Figure 10 shows part of the deformed mesh, for a uniform temperature change of -90K. The manufacturers' data sheet for AV119 states a cure temperature of 110°C and this figure has been used here (a lower figure has been used elsewhere [11]). The strain profile in figure 11 shows the elastic strain in the longitudinal direction, EE11, in the bonded part of the joint (which is the elastic strain that results from bonding the adherends) to be -820 με, which is in good agreement with the measured strain of -810 με found experimentally (see section 3.1).

Disbonds are modelled as seams (uncoupling of nodes common to two elements) between the adhesive and the GFRP (which is the position of the disbonds found experimentally). Disbonds of 5 and 10 mm have been modelled, in one case with the disbonds starting at the termination of the aluminium adherend and in the other case with the disbonds starting at the termination of the GFRP adherend (corresponding to the low wavelength and high wavelength end of the CFBG, respectively).

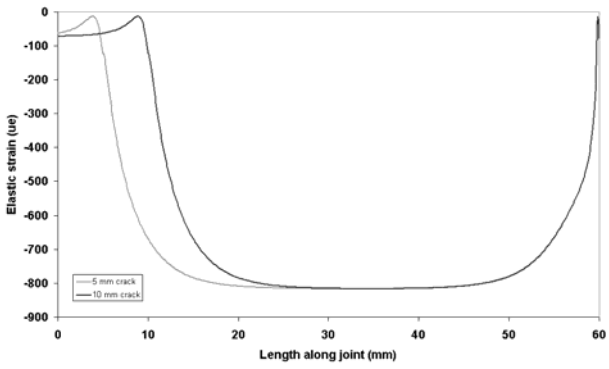

Fig. 11 Elastic strain profiles in the GFRP for 5 and 10 mm disbonds from the aluminium adherend termination

The longitudinal elastic strain profiles at the approximate position of the sensor are shown in figure 11, which has disbonds originating from the aluminium adherend termination. These strain profiles are taken along a line of nodes indicated by the "A" in figure 10. This line is 0.375 mm from the bond line of the GFRP adherend, which is close to the nominal position of the centreline of the optical fibre. The strain profiles have been used to calculate the grating period of the CFBG sensor [9] which has then been used in OptiGrating software (Optiwave corporation, Canada) to predict the reflected spectra. Predicted spectra for 5 mm and 10 mm disbonds initiating at the aluminium adherend termination are shown in figure 12. In the spectra, the vertical lines represent the actual position of the disbond front in the model. The predicted spectra show that the disbond front is adjacent to the base of the intensity peak, i.e. the peak of the perturbation is in advance of the actual disbond front by about 1 mm. The shapes of the predicted spectra are in good agreement with the experimental results (figure 6).

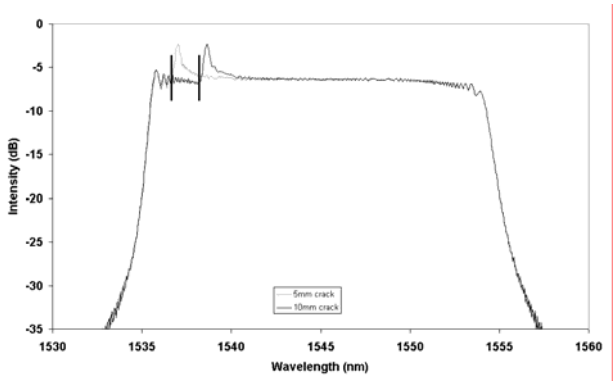

Fig. 12 Predicted spectra for 5 and 10 mm disbonds at the low wavelength end of the CFBG

The strain profile and predicted spectra for a disbond initiating at the GFRP adherend termination are shown in figures 13 and 14, respectively. The more complicated form of the strain profile is caused by end effects within the model. Again, the vertical lines in the spectra in figure 14 are the actual positions of the disbond front in the model. The position of the disbond front at the high wavelength end is less well defined than the low-wavelength end, being in the middle of the downward slope of the perturbation. Again, the minimum of the dip in the spectra is in advance of the actual disbond position, this time by about 1.5 mm. The shapes of the predicted spectra are again

in good agreement with the experimentally determined spectra (figure 8).

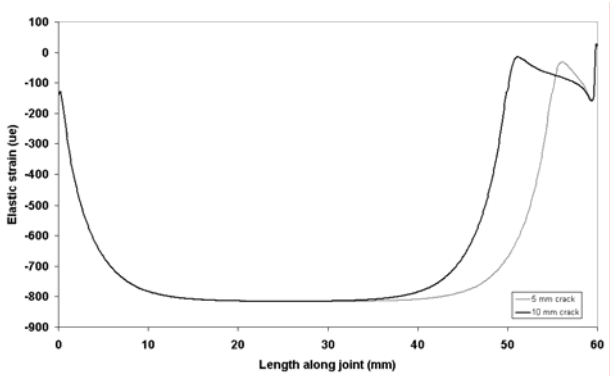

Fig. 13 Elastic strain profiles for 5 and 10 mm disbonds from the GFRP adherend termination

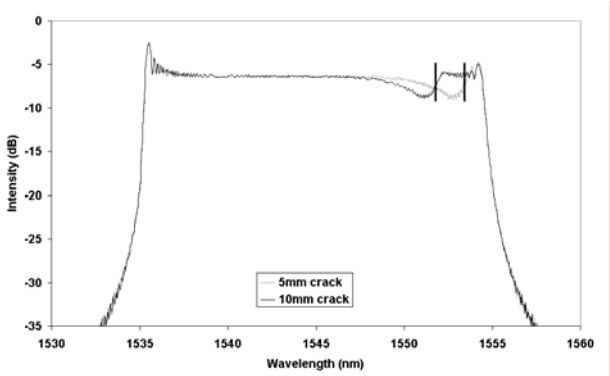

Fig. 14 Predicted spectra for 5 and 10 mm disbonds at the high wavelength end of the CFBG

4 Conclusions

This paper has reported the use of chirped fibre Bragg grating for monitoring disbonds in metal/composite single lap joints. The technique makes use of the thermal mismatch strain locked into the joint at manufacture, due to the different coefficients of thermal expansion of the two adherend materials. It has been shown that initiation of the disbond results in a distinct change in the reflected spectrum from the sensor and that subsequent growth of the disbonds can be monitored to within about 2 mm. Numerical modelling has also been presented that supports the experimental results.

References

[1] Hsu D, "Nondestructive testing using air-borne ultrasound", *Ultrasonics*, Vol 44, e1019-1024, 2006

[2] Schroeder JA, Ahmed T, Chaudhry B, Shepard S "Non-destructive testing of structural composites and adhesively bonded composite joints: pulsed thermography", *Composites part* A, Vol 33, pp 1511-1517, 2002

[3] Omar M, Hassan M, Donohue K, Saito K, Alloo R, "Infrared thermography for inspecting the adhesion integrity of plastic welded joints", *NDT&E International*, Vol 39, pp1-7, 2006

[4] Forsyth DS, Genest M, Shaver J, Mills T, "Evaluation of nondestructive testing methods for the detection of fretting damage", *International Journal of Fatigue*, Vol 29, pp810–821, 2007

[5] Paget CA, "Modified AE for structural damage monitoring of complex structures", *Proceedings of SAA "Structural Validation and Health Monitoring of Adhesive Joints"*, 19th April 2007

[6] Takeda S, Aoki Y, Ishikawa T, Takeda N, Kikukawa H, "Structural health monitoring of composite wing structure during durability test", *Composite Structures*, Vol 79, pp133-139, 2007

[7] Li HCH, Herszberg I, Davis CE, Mouritz AP, Galea SC, "Health monitoring of marine composite joints using fibre optic sensors", *Composite Structures*, Vol 75, pp321-327, 2006

[8] Okabe Y, Tsuji R, Takeda N, "Application of chirped fiber Bragg grating sensors for identification of crack locations in composites", *Composites Part A*, Vol 35, pp59-65, 2004

[9] Yashiro S, Okabe T, Takeda N, "Damage detection in a holed CFRP laminate using a chirped fibre Bragg grating sensor", *Composite Measurements Science and Technology,* Vol 67, pp286-295, 2006

[10] Palaniappan J, Wang H, Ogin S L, Thorne A M, Reed G T, Crocombe A D and Tjin S C, "Structural health monitoring of bonded composite joints using embedded chirped fibre Bragg gratings", *Advanced Composites Letters,* Vol 14/6, pp185-192, 2005

[11] Capell TF, Palaniappan J, Ogin SL, Crocombe AD, Reed GT, Thorne AM, Mohanty L, Tjin SC, "The use of an embedded chirped fibre Bragg grating sensor to monitor disbond initiation and growth in adhesively bonded composite/metal single lap joints", *Journal of Optics A*, Vol 9, 2007, In Press

[12] Palaniappan J, Unpublished work, 2006